ISSN 2176-5480

22nd International Congress of Mechanical Engineering (COBEM 2013)
November 3-7, 2013, Ribeirão Preto, SP, Brazil

THE INTERFERENCE OF ROOF PROFILE ON WIND FIELDS OF INDUSTRIAL BUILDINGS

Bianca Hulle de Souza
Department of Mechanical Technical, IFES, Vitoria, Espirito Santo, Brazil
biancahulles@hotmail.com

Fernanda Capucho Cezana
Department of Mathematical, IFES, Vitoria, Espirito Santo, Brazil
fe.cezana@gmail.com

Reginaldo Rosa Cotto de Paula
Marcela Pimenta Brito
Department of Sanitary and Environmental Engineering, IFES, Vitoria, Espirito Santo, Brazil
cottoreginaldo@gmail.com; marcelampb.sa@gmail.com

Marcos Sebastião de Paula Gomes
Mechanical Engineering Department, PUC-RIO, Rio de Janeiro, Brazil
mspgomes@mec.puc-rio.br

Abstract. *The objective of this study was to investigate experimentally the effect of different roof shapes of scale model industrial buildings on wind flow. The analysis was performed by means of atmospheric wind tunnel experiments with three roof shapes: shed, arc and slanted. A flow visualization technique was applied to investigate the influence of the roof shapes on wind flow at different Reynolds numbers. Smoke was used as the tracer gas and it was generated by a smoke machine (LS1500W). The scale model building was illuminated using a 500 mW Green Laser Module by passing a beam of laser light through a semicylindrical lens. The incident wind angle was perpendicular to the frontal face of the scale model industrial building. In the general the results presented no significant differences on the vortex structures at the frontal and back faces of the different buildings. However, the results showed that flow structures at the top were strongly dependent on the roof profile.*

Keywords: *roof profile, wind tunnel experiments, flow visualization*

1. INTRODUCTION

Isolated buildings have received much attention and there is well detailed information about the vortex structures and the complexities induced in the flow around buildings with flat roofs, such as cubical and rectangular buildings (Stathopoulos and Zhou, 1995; Richards and Hoxey, 2006; Tominaga *et al*., 2008). However, wind flow around buildings is greatly affected by the roof profile (Rafailids, 1997).

Flow field characteristics over shed, arc and slanted roof building models have been experimentally investigated, allowing a quantification of the effects of different roof profiles on the wind flow in the neighborhood of the buildings. However, this remains a difficult task for accurate experimental investigation (Lien and Ahmed, 2011), because the flow patterns that develop at roof level present high turbulence, severe pressure gradients, flow separation and possible flow reattachment. and in addition, in the near wake the mean flow is affected by separating shear layer and vortices shed from the upstream building edges. while the mean wind decreases and the turbulence increases in the direction of the flow. In the far wake the effects of building on the wind flow field decay (Hosker, 1981).).

Thus, the knowledge of the influence of roof shape on wind flow is of interest because of several building and urban engineering purposes. Raifalidis (1997) analyzed in a wind tunnel the flow characteristics in the lower part of the atmospheric boundary layer above a building roof in a model urban fetch.The author found that the wind flow and turbulence intensity at the roof level was strongly dependant on the roof profile He suggested that altering the roof shape can have a much more beneficial impact on urban air quality than increasing the spacing between buildings.

Franchini et al. (2005) investigated experimentally the effects of conical vortices on the wind loads generated on curved roofs and the influence of the roof curvature on the wind-induced mean pressure distribution on a low building's roof. The results indicate that roof curvature modifies both the magnitude of mean suction peaks and their positions on the roof.

Suaris and Irwin (2010) conducted tests in a boundary layer wind tunnel to investigate the effectiveness of parapets mounted at the roof-edge in mitigating the high intermittent suctions near corners of low rise building roofs. The results indicated that the localized peak pressure coefficient for the corner zone was about -9.5 for the test without any parapets

ISSN 2176-5480

somewhat higher than the values obtained by others with smaller models with lower Reynolds numbers. In the corner zone the peak pressure coefficients were reduced by over 50% by the placement of parapets along the perimeter. In addition, the authors concluded that the perforated parapets with a perforation ration of 33% having a length of 10% of the shorter building dimension installed at the corners and at the ridge resulted in about 60% reduction in the peak pressure coefficients at the corners.

The main objective of this study was to analyze experimentally the effect of different roof profiles of scale model industrial buildings on the wind flow. The analysis was performed in atmospheric wind tunnel experiments with three roof shapes: shed, arc and slanted. Flow visualization technique was applied to investigate the influence of the roof shapes on wind flow at different Reynolds numbers.

2. MATERIAL AND METHODS

The flow considered in this work was investigated in an open return wind tunnel with a test section 2.0 m long, 0.5 high and 0.5 wide, in the Energy Laboratory of IFES, Vitoria, Brazil. An atmospheric boundary layer was generated by various spires and roughness elements made with wood which were installed upwind of the test area of the wind tunnel to generate a neutral atmospheric boundary layer with δ = 0.3 m deep. The dimensions and spacing of spires and roughness elements were calculated using the methodology proposed by Irwin (1981). The mean velocity upstream of the industrial scale model building at an elevation z = 1.0 H_b, where H_b is the building height, was used to categorize the flow field. The mean streamwise velocity has the following power law profile:

$$\frac{U(z)}{U_\delta} = \left(\frac{y}{\delta}\right)^p \tag{1}$$

The velocity profile was fitted with p = 0.30 which corresponds to the velocity profile over suburban sites (Blessman, 1995). Smoke flow technique was used to visualize the wind flow around the industrial building. Fluid from a smoke machine (LASER DJ 1500w) was generated and injected into the wind tunnel through a pipe (50 mm diameter), with the industrial building downstream of the outflow. A green laser light passing through a spinning cylindrical lens was used to illuminate the vicinity of the building to facilitate a clear visualization of the vortex system and permit quantitative analysis of the wind flow. A diode laser module of operating at 500 mW (532 nm) was mounted outside the wind tunnel in the center line and elevated to approximately 170.0 cm. A digital camera (Fujifilm HS 10) was used to record the smoke patterns at a speed of 240 frames per second (fps). The camera was placed outside the wind tunnel looking through either side. Selected sequences of video pictures were both digitally and visually studied. Three building models, with the same plan dimensions but different roof profiles (shed, arc and slanted) were used in the wind tunnel experiments. The building models, with external dimensions of 0.150 m (width) by 0.300 m (length) and 0.120 m (height, H_b) (1/100) were as shown Fig. 1.

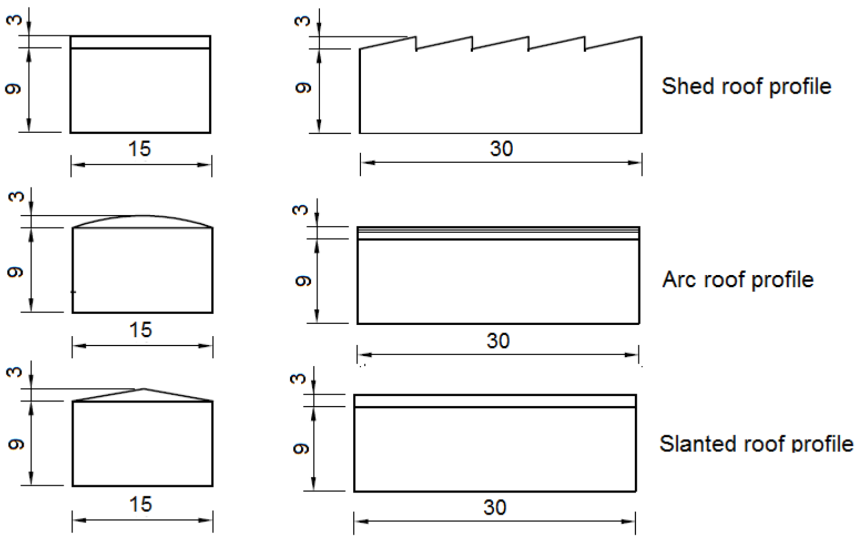

Figure 1. Sketch of industrial building models with different roof profiles.

In this work the Reynolds numbers were based on building height H and wind velocity at the building height, U_h. In addition there were used air density of 1.185 kg/m^3 and air viscosity of 1.82 × 10^{-5} kg / m^2.s. Table 1 shows the measurements of the mean wind velocity at building height and correspondent Reynolds number.

ISSN 2176-5480

Table 1. Results of measurements of the mean wind velocity at building height and Re numbers.

U_h (m/s)	Re
0.31	2409
0.64	4975
1.40	10883

3. RESULTS

The present paper describes investigation of the flow around industrial scale model buildings in an atmospheric boundary layer wind tunnel. The flow pattern and the vortex structure were studied by using buildings of the same dimensions but, with different roof profiles and different Re numbers.

3.1 – Incident region

Figures 2-4 shows the results of flow visualization in a section normal to the flow in the incident region of a building with the shed roof profile used in this work. On reaching the frontal face of the building, the air flow decelerated longitudinally and accelerated vertically to pass around it. Thusly, the oncoming flow impinged on the frontal face of obstacle and the fluid flow went toward the ground and returned in the direction opposite to the main flow. In this way, a reverse flow was created in the incident flow region and at same time a standing vortex was generated due to the interaction between the flowstream and the reverse flow.

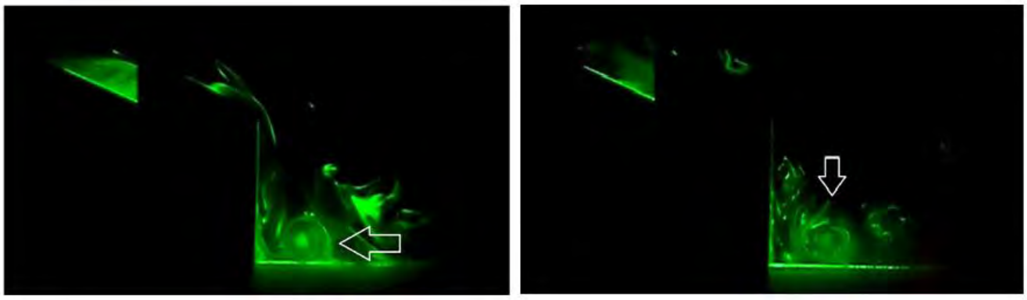

Figure 2. Side view: Laser-sheet visualization of the flow in front of a building with shed roof for Re = 2490.

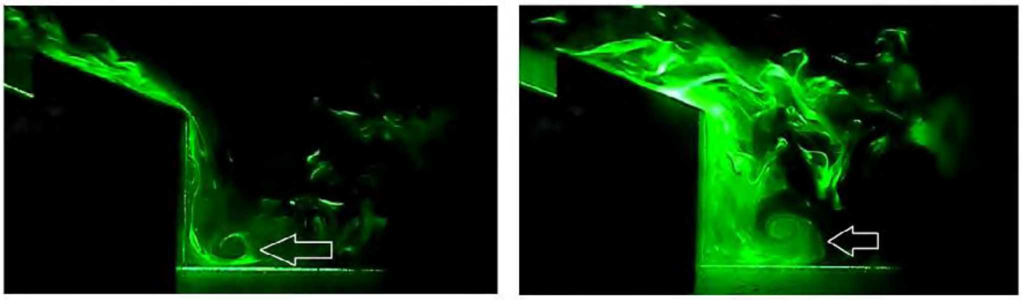

Figure 3. Side view: Laser-sheet visualization of the flow in front of a building with shed roof for Re = 4975.

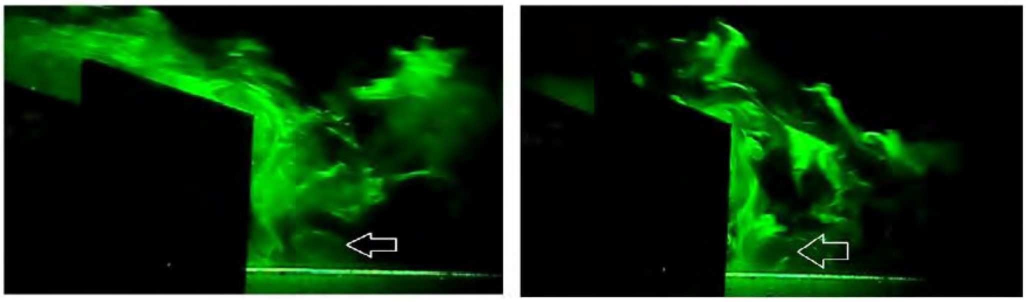

Figure 4. Side view: Laser-sheet visualization of the flow in front of a building with shed roof for Re = 10882.

Flow visualization results in a section normal to the flow upwind of the frontal face of building with an arc roof is shown in Figs. 5 – 7. The flow reattached on the front face of the obstacle, at the upwind stagnation point. In this case there was also observed the formation of a standing horizontally oriented vortex near the ground upwind of the frontal face of building.

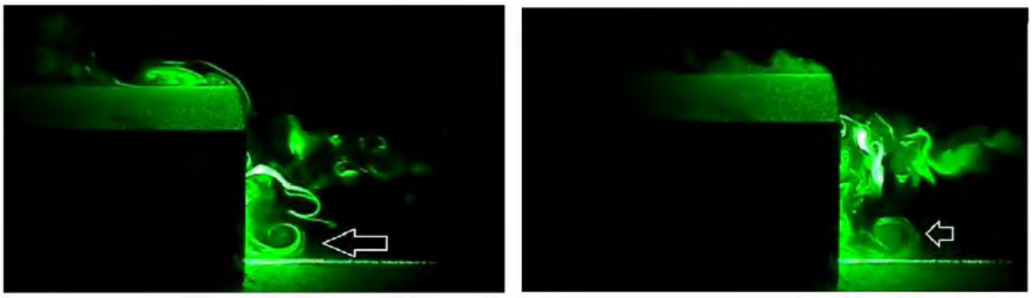

Figure 5. Side view: Laser-sheet visualization of the flow in front of a building with arc roof for Re = 2490.

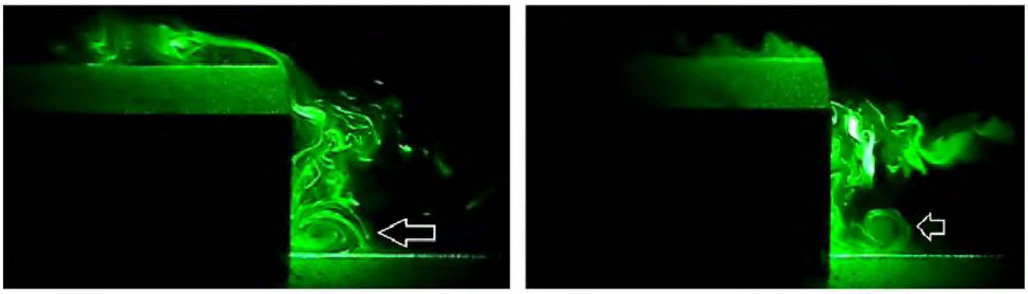

Figure 6. Side view: Laser-sheet visualization of the flow in front of a building with arc roof for Re = 4975.

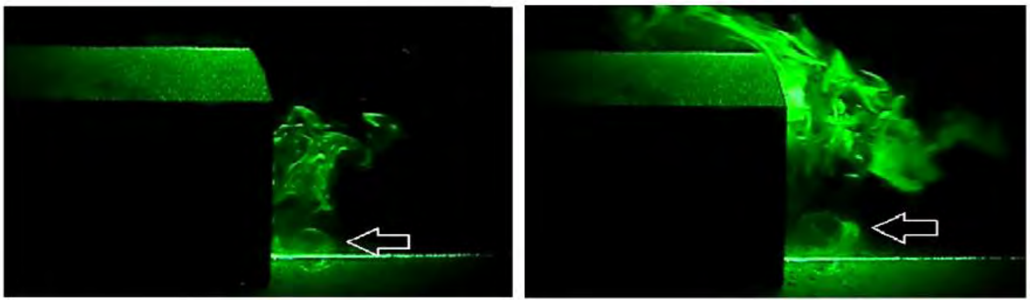

Figure 7. Side view: Laser-sheet visualization of the flow in front of a building with arc roof for Re = 10882.

Qualitatively comparing pictures of the incident region for the different buildings, it turned out that there was no fundamental change in the vortex structure on the ground, as show the Figs. 8 – 10 for building with a slanted roof. Also, a roll standing vortex was generated at the frontal face of the building with a slanted roof.

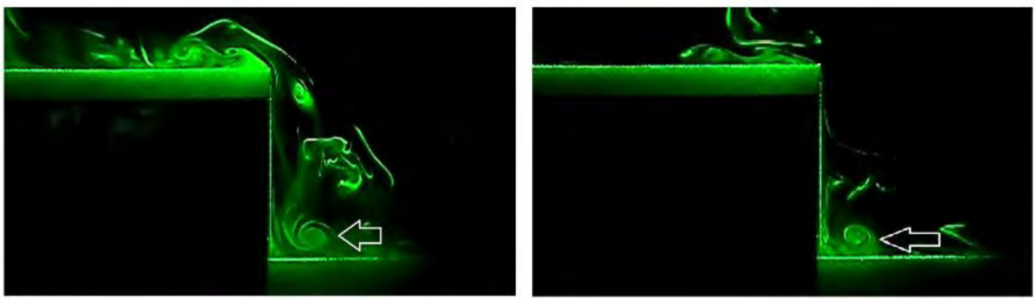

Figure 8. Side view: Laser-sheet visualization of the flow in front of a building with slanted roof for Re = 2490.

ISSN 2176-5480

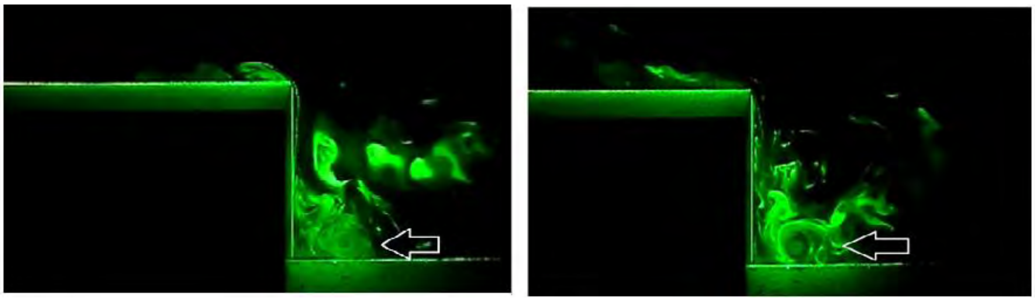

Figure 9. Side view: Laser-sheet visualization of the flow in front of a building with slanted roof for Re = 4975.

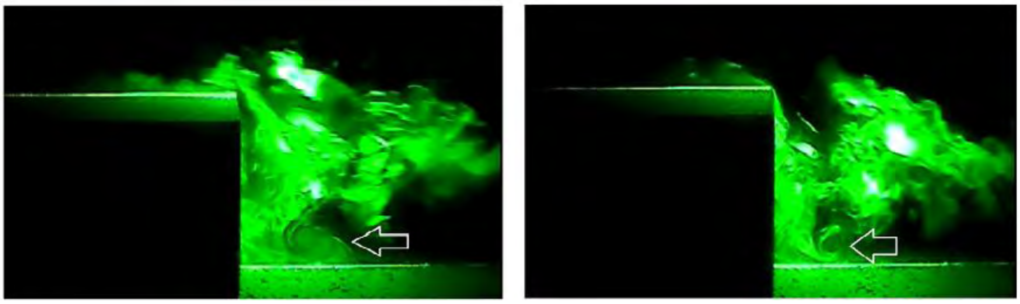

Figure 10. Laser-sheet visualization of the flow in front of a building with slanted roof for Re = 10882.

3.2 – Roof of buildings

Figures 11-13 show results of the flow visualization above the shed roof building. The flow was vertically accelerated when it impinged on the frontal face of the building. Thusly, the flow separated the boundary layer from the edges of the frontal wall and reattached it to the roof of the building. This region was characterized by circulatory motion, low flow velocities and high turbulence. In addition to the effect of the inclined roof on wind flow there was observed the formation of a shedding vortex within the cavities of the roof region at the windward face, as seen in Figs. 11-13.

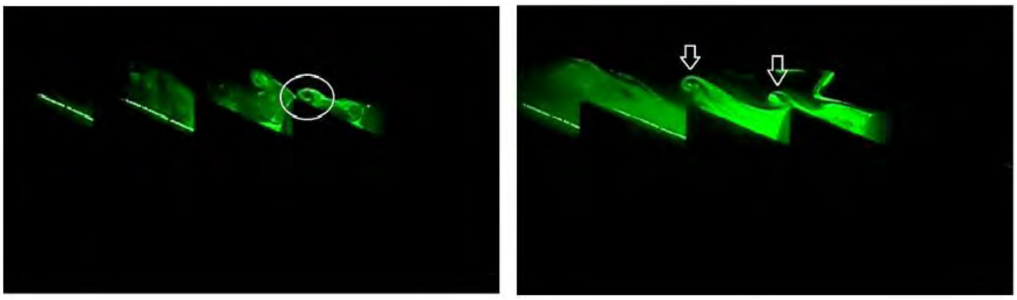

Figure 11. Side view: Laser-sheet visualization of the flow on shed roof for Re = 2490.

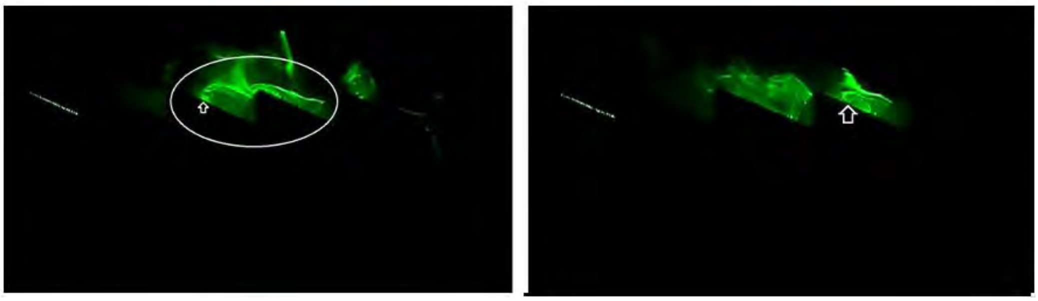

Figure 12. Side view: Laser-sheet visualization of the flow on shed roof for Re = 4975.

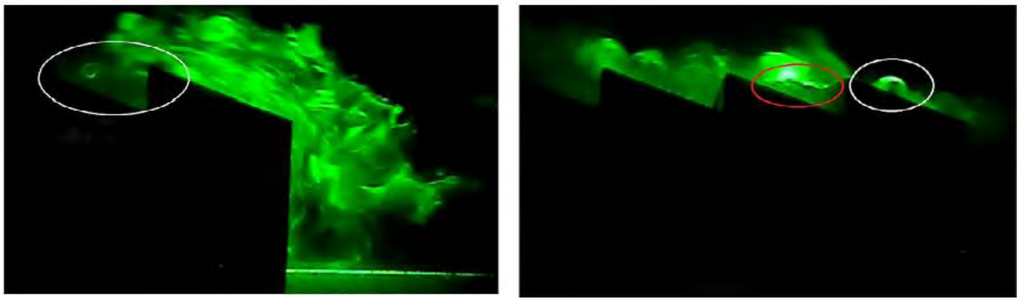

Figure 13. Side view: Laser-sheet visualization of the flow on shed roof for Re = 10882.

Figures 14-19 display pictures of the features of flow over buildings with arc and slanted roofs. The flow separated at the top of the windward wall and reattached at a region further downwind on the roof, which caused the formation of a recirculation. This region was bounded by a free shear layer, a region of high turbulence. This layer rolls up intermittently to form vortices. The effect this turbulence on the approaching flow was to cause the vortices to roll closer to the leading edge, and produce a shorter distance to reattachment on the roof.

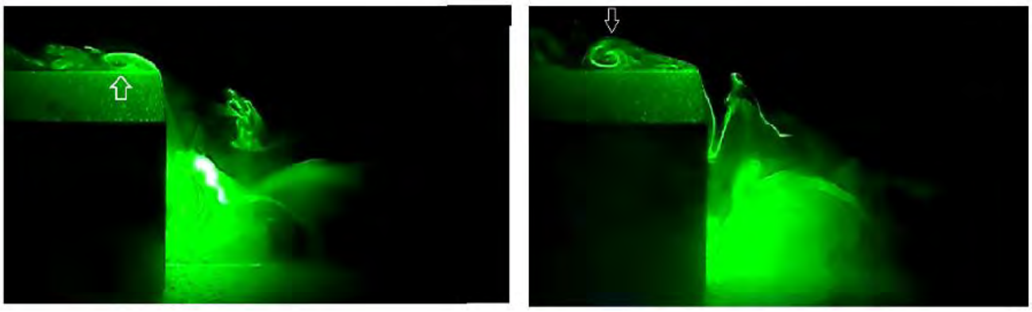

Figure 14. Laser-sheet visualization of the flow on arc roof for Re = 2490.

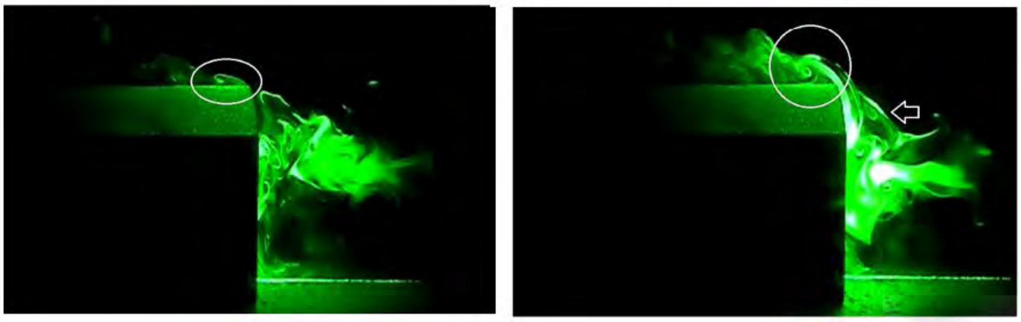

Figure 15. Laser-sheet visualization of the flow on arc roof for Re = 4975.

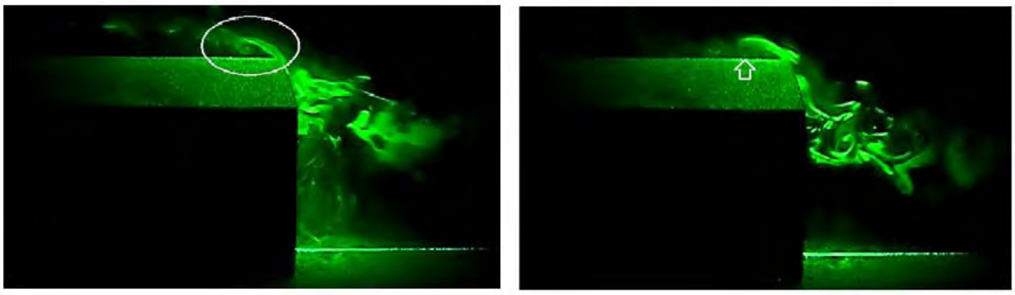

Figure 16. Laser-sheet visualization of the flow on arc roof for Re = 10882.

ISSN 2176-5480

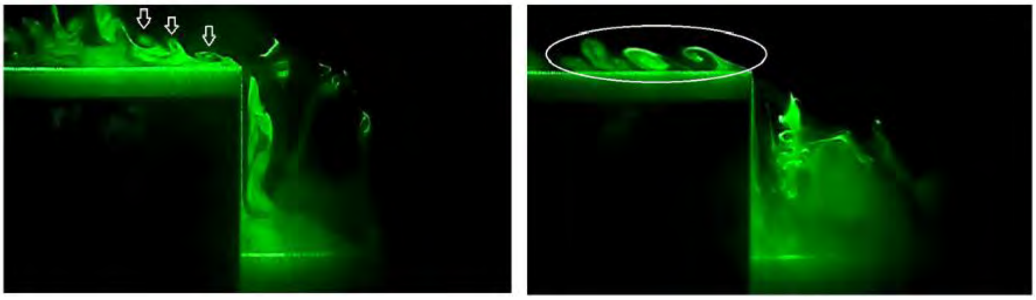

Figure 17. Laser-sheet visualization of the flow on slanted roof for Re = 2490.

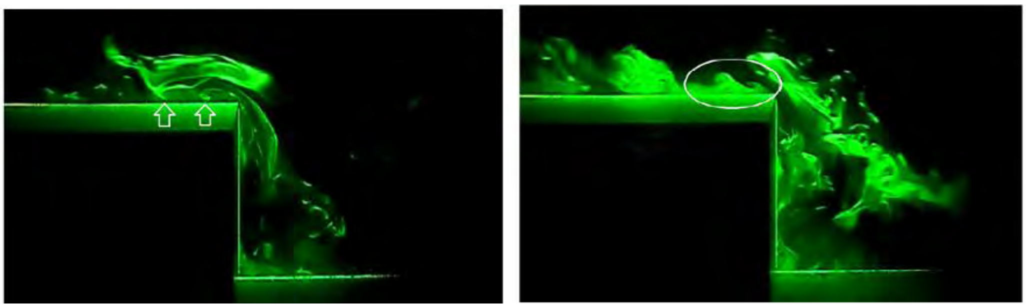

Figure 18. Laser-sheet visualization of the flow on slanted roof for Re = 4975.

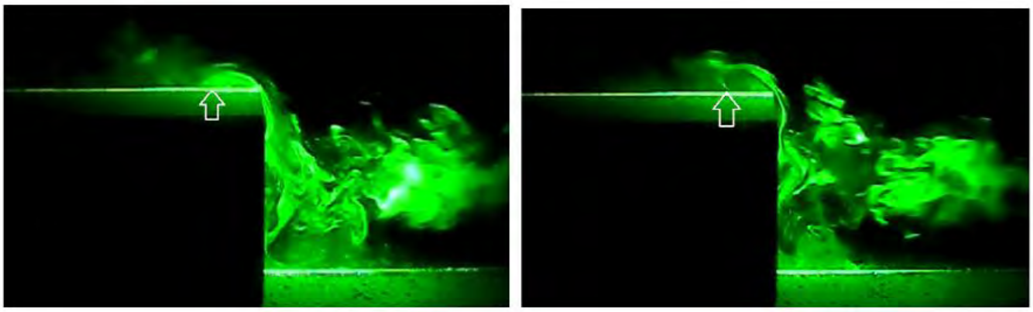

Figure 19. Laser-sheet visualization of the flow on slanted roof for Re = 10882.

3.3 – Near wake results

Figures 20-28 display pictures of flow in the near wake for all buildings and Reynolds numbers investigated in this work. The results showed that in the near wake the mean flow and turbulence intensity were affected by separating shear layers and vortices shed from the upstream building edges. The vortex shedding was detected at the edge near the top of leeward wall. In near wake the mean wind decreases and the turbulence increases in the direction of the flow. In addition, qualitatively the near wake may have a length up to a few building heights. Qualitatively comparing pictures for different near wake formations, it turned out that there was no fundamental change in the vortex structure in this zone.

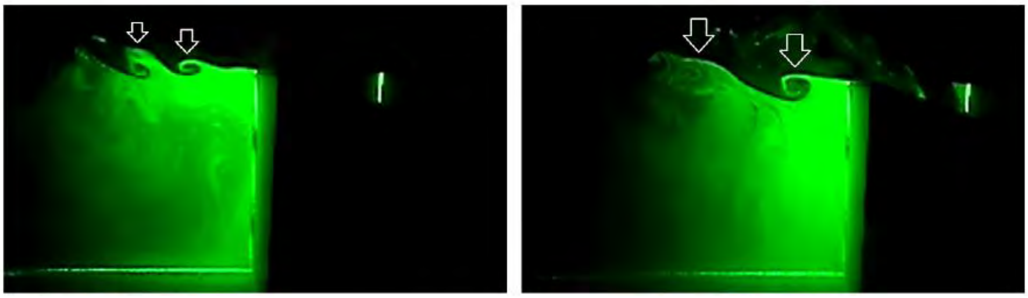

Figure 20. Side view: Laser-sheet visualization on the flow in near wake of shed roof building for Re = 2490.

ISSN 2176-5480

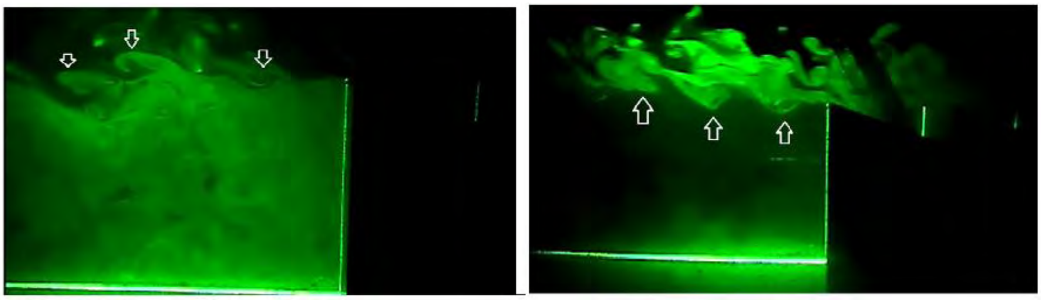

Figure 21. Side view: Laser-sheet visualization of the flow in near wake of shed roof building for Re = 4975.

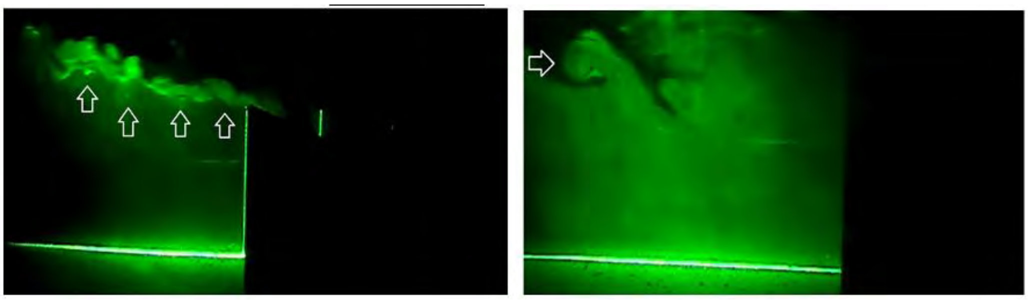

Figure 22. Side view: Laser-sheet visualization of the flow in near wake of shed roof building for Re = 10882.

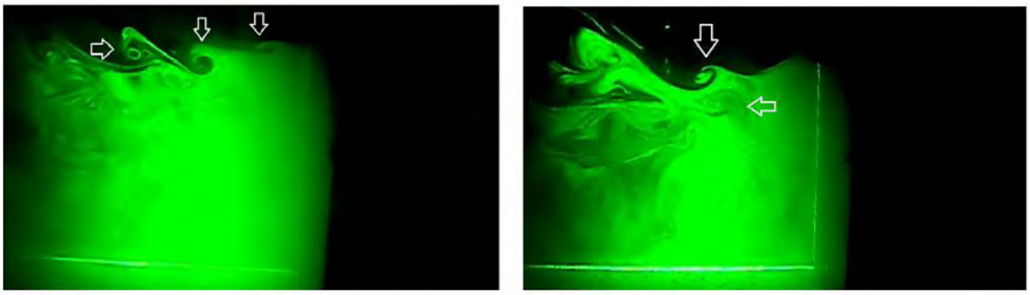

Figure 23. Side view: Laser-sheet visualization of the flow in near wake of arc roof building for Re = 2490.

Figure 24. Side view: Laser-sheet visualization of the flow in near wake of arc roof building for Re = 4975.

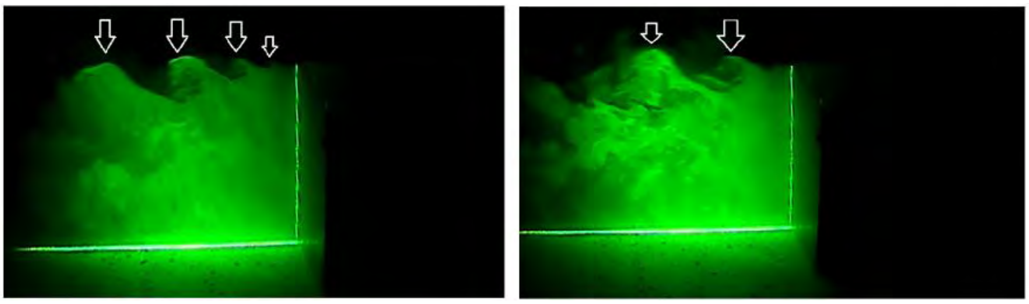

Figure 25. Side view: Laser-sheet visualization of the flow in near wake of arc roof building for Re = 10882.

ISSN 2176-5480

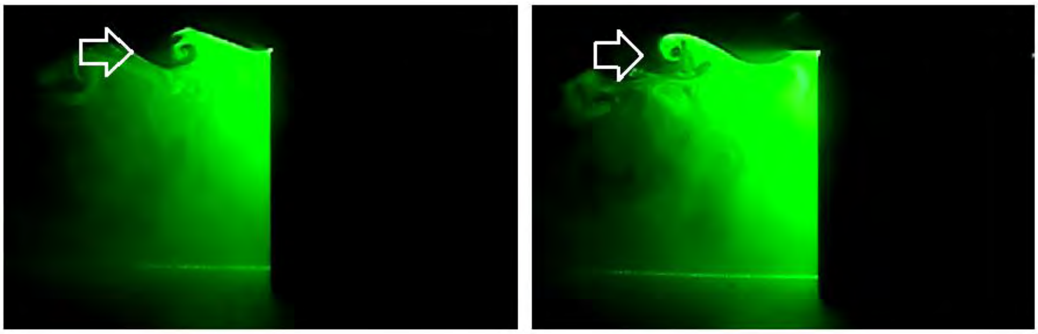

Figure 26. Side view: Laser-sheet visualization of the flow in near wake of slanted roof building for Re = 2490.

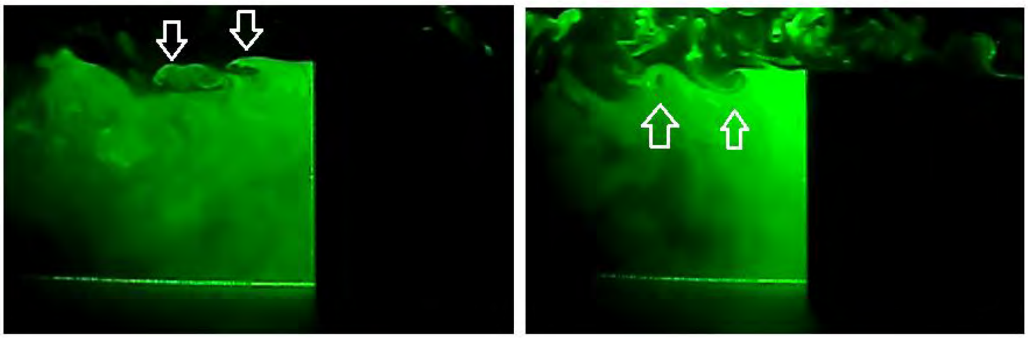

Figure 27. Side view: Laser-sheet visualization of the flow in near wake of slanted roof building for Re = 4975.

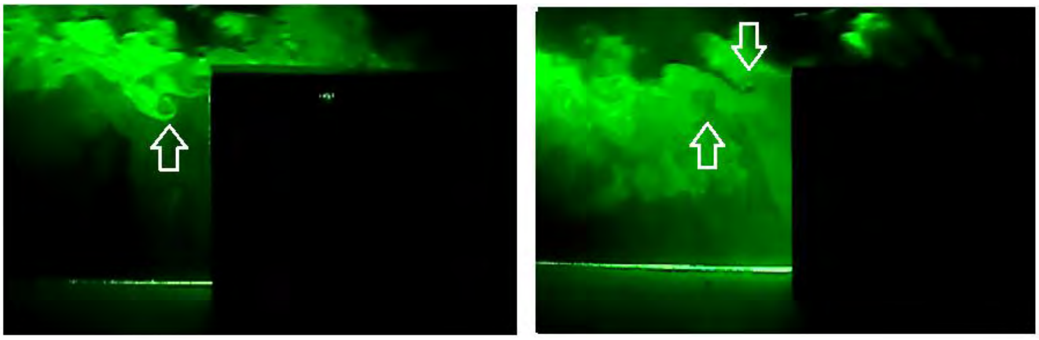

Figure 28. Side view: Laser-sheet visualization of the flow in near wake of slanted roof building for Re = 10882.

3.4 – Horseshoe vortex near building with slanted roof

The horseshoe vortex that forms around the base of the rectangular building is clearly visible in Fig. 29. This vortex system at the frontal and lateral wall of the obstacles was caused by the adverse pressure gradient of the stagnating flow (Hosker, 1981).

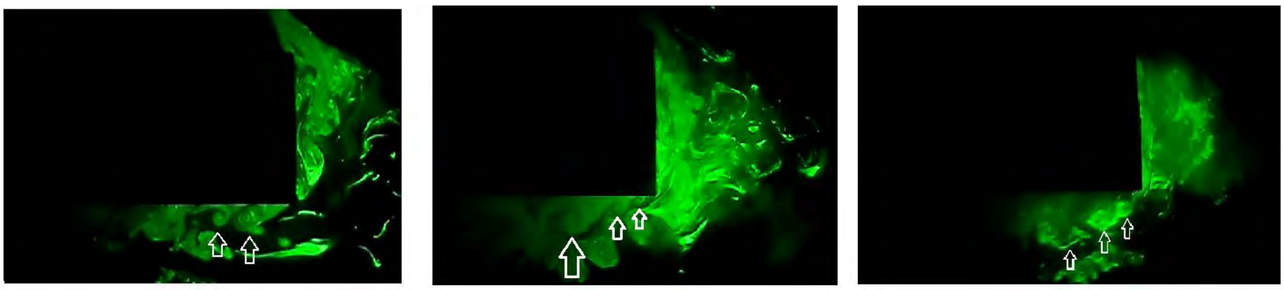

(a) (b) (c)

Figure 29. Flow visualization at x-y plane of the horseshoe vortex system around building with slanted roof at z = 0.02 m: (a) Re = 2490; (b) Re = 4975 and (c) Re = 10882.

4. CONCLUSIONS

Flow visualization with the smoke injection technique was performed and gave qualitative characteristics of flow structure around isolated buildings. At the frontal face of buildings there was observed a standing vortex and by the lateral wall, near the ground, the horseshoe vortex. This finding shows that a flow with separation on the upstream edge of building can induce a reattachment point and recirculation region on arc and slanted roof profiles. In the near wake the flow was affected by separating shear layer and shedding vortex formation near the edge on the top behind the building. The general results no presented significant differences in vortex structures in front of and behind the faces of buildings. However, the results showed that flow structure on top was strongly dependent on the roof profile.

The results showed that the patterns of fluid flow around buildings were very complex, with three-dimensional turbulent structures produced by the shear stress of the wind flow when disturbed by the building. In this work the flow patterns were considered to be affected by only by the shear stress, and thus, no buoyancy forces were recognized. Despite the complexity of this mechanism was possible to identify characteristics of the flow system around buildings such as standing vortex, horseshoe vortex, reattachment point and recirculation region on the roof as well as shedding vortex and near wake formation.

5. ACKNOWLEDGEMENTS

The authors would like to acknowledge the financial support from CNPq and Mechanical Technical Department of IFES, Vitoria, Espirito Santo, Brazil

6. REFERENCES

Blessmann, J., 1995. “O vento na Engenharia Estrutural”. Editora Universidade, Universidade Federal do Rio Grande do Sul.

Franchini, S., Pindado, S., Meseguer, J. Sanz-Andre´ s, A., 2005. “A parametric,experimental analysis of conical vortices on curved roofs of low-rise buildings”. *Journal of Wind Engineering and Industrial Aerodynamics*, Vol. 93, pp. 639–650.

Hosker, Jr., R.P., 1981, “Methods for estimating wake flow and effluent dispersion near simple block-like building”, NOOA, National Oceanic and Atmospheric Administration, NOAA Technical Memorandum ERL ARL-108.

Irwin, H.P., 1981. “The Design of Spires for Wind Simulation”. Journal of Wind Engineering and Industrial Aerodynamics, Vol. 7, pp. 361-366.

Lien, S.T. and Ahmed, N.A., 2001. “Effect of inclined roof on the airflow associated with a wind driven turbine Ventilator”. Energy and Building, Vol. 43, pp. 358-365.

Richards, P.J. and Hoxey, R.P., 2006. “Flow reattachment on the roof of a 6 m cube”. *Journal of Wind Engineering and Industrial Aerodynmics*, Vol. 99, pp. 77-99.

Rafailidis S., 1997. “Influence of building areal density and roof shape on the wind characteristics above a town”. *Boundary Layer Meteorology*, Vol. 85, pp. 55-71.

Stathopoulos, T. and Zhou, Y.S., 1996. “Numerical evaluation of wind pressures on flat roofs with the κ-ε model”. Building Environment, Vol. 30, pp. 267-276.

Suaris, W., and Irwin, P., 2010. “Effect of roof-edge parapets on mitigatin extreme roof suctions”. *Journal of Wind Engineering and Industrial Aerodynmics*, Vol. 98, pp. 483-491.

Tominaga, Y., Mochida, A., Murakami, S. and Sawaki, S., 2008. “Comparison of various revised k–3 models and LES applied to flow around a high-rise building model with 1:1:2 shape placed within the surface boundary layer”. *Journal of Wind Engineering and Industrial Aerodynamics*, Vol. 96, pp. 389–411.

7. RESPONSIBILITY NOTICE